The Effect of Prey Surface Roughness on the Viscous Adhesion Force of Frog Saliva

A Major Qualifying Project Report
Submitted to the Faculty of
WORCESTER POLYTECHNIC INSTITUTE
in partial fulfillment of the requirements for the
Degrees of Bachelor of Science
in
Physics and Mechanical Engineering
By
Ana Gabriela Cano Zimmerman
August, 2021

Many thanks to the advisors this project is being submitted to,
I am grateful for their patient help and unwavering support.
This project could not have been completed without them:

Ahmet Can Sabuncu, *Advisor in Mechanical Engineering*
Izabela RC Stroe, *Advisor in Physics*
Aswin Gnanaskandan, *Co-Advisor in Mechanical Engineering*

Abstract

The frog uses wet adhesion and a soft tongue in order to capture its prey. This swift capture, unmatched by known synthetic mechanisms, benefits from being understood in its totality. The adhesion is due to a frog's shear thinning saliva, which can be treated as a high viscosity Newtonian fluid under low shear stress and a low viscosity Newtonian fluid under high shear stress. With shear forces playing a large role, it follows that the texture of the surface could impact the adhesive strength of the tongue. An experiment was designed using dynamic similarity to determine the impact surface roughness has on the adhesive properties of the frog tongue. The experiments did not reveal any significant impact of surface roughness on the adhesive strength of the bond between tongue and prey.

Index

List of Figures 3
List of Tables 3
1. Literature Review 4
1.1 The Mechanics of Prey Capture in the Frog 4
1.2 The Role of Saliva in The Frog's Incredibly Sticky Tongue 4
1.3 The Shear-Thinning Saliva of Frogs: A Newtonian Approach to A Non-Newtonian Flow 5
1.4 An Overview of Dimensional Analysis 5
1.5 The Non-Dimensional Navier-Stokes Equation 6
1.6 The Non-Dimensional Boundary Conditions 7
1.7 Adhesive Bond Strength Testing 7
1.8 Sandpaper Roughness Values 8
2. Experimental Methods 8
2.1 Materials 8
2.2 Numerical Values 9
2.3 Plate Construction 10
2.4 Plate Separation Device Construction 11
2.5 Sample Preparation and Testing 12
2.6 Video Analysis 12
3. Results and Discussion 13
3.1 Generalized Flow Behavior 13
3.2 Impact of Surface Roughness 14
3.3 Sources of Error 16
4. Conclusion 16

List of Figures

Figure 1: Tongue Projection and Retraction of the Horned Frog 4
Figure 2: Viscosity vs. Shear Rate Graph of Frog Saliva 5
Figure 3: Exterior of plate separation device at maximum separation. 11
Figure 5: Velocity-time curve, 80 grit first trial. 13
Figure 6: Acceleration-time curve, 80 grit first trial. 13
Figure 7: Velocity-time curve, no adhesion. 14
Figure 8: Acceleration-displacement curve, 80 grit first trial. 14
Figure 9: Mean Work of Adhesion vs. Arithmetic Mean Surface Roughness 15

List of Tables

Table 1: Grit Value and Corresponding Arithmetic Mean of Height Deviations from Main Line (Ra) ... 8
Table 2: Materials and Their Purposes 8
Table 3: Weber Number Inputs, Real World Data 9
Table 4: Froude and Reynolds Number Variable Inputs 10
Table 5: Froude and Reynolds Number Constant Inputs 10
Table 6: Froude and Reynolds Number at Impact and Retraction 10
Table 7: Summary of Collected Data 15
Table 8: Summary of Analysis of Variables 16

1. Literature Review

1.1 The Mechanics of Prey Capture in the Frog

The tongue of the frog is unmatched in grabbing speed by any commercial mechanism (reaching accelerations of 120 m/s^2) and fifty times greater work of adhesion than any known synthetic polymer materials.[1] This is due to a combination of non-Newtonian shear-thinning saliva coating a soft, viscoelastic tongue.[2]

Frogs' tongues are attached at the front of the mouth as seen in Figure 1 and are shot out at prey like sling shots. In some frog species this is done through muscle power alone, but others, like the horned frog, rapidly depress their lower jaw in conjunction to generate even greater speed.[3]

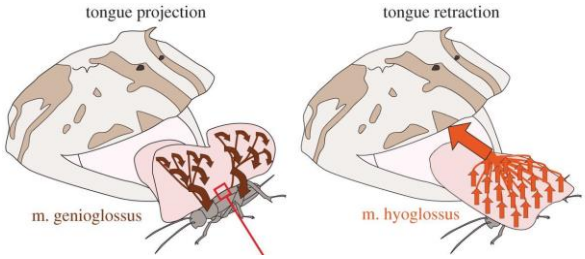

Figure 1: Tongue Projection and Retraction of the Horned Frog[3]

The tongue acts as a shock absorber, preventing separation of saliva from the insect as it experiences up to over 12 g's of acceleration.[1] The softer a material tongue, the more it can stretch and absorb impact, and the frog's tongue is one of the softest known biological materials.[2] Additionally, its viscoelastic properties allow it to stretch with the saliva layer, retaining contact with the insect in fibrils even if other sections of tissue have detached.

1.2 The Role of Saliva in The Frog's Incredibly Sticky Tongue

The frog's saliva is shear thinning: it becomes less viscous under shear stress. Forces acting parallel to the saliva layer cause the saliva to flow easily, while forces acting perpendicular do not.[2] Impact speeds of the tongue reach well over the limit at which saliva begins to flow with ease, which allows the saliva to flow over the surface of prey on impact and become incredibly viscous and thus sticky upon retraction.[1]

In order to remove the prey from its tongue, the frog must once again apply shear stress. This is done by retracting the eyes into the oral cavity, effectively scraping the prey off the tongue, and pushing it down toward the stomach.[1]

1.3 The Shear-Thinning Saliva of Frogs: A Newtonian Approach to A Non-Newtonian Flow

Frog saliva obeys the Carreau Yasuda model for a shear thinning fluid in which the viscosity of the fluid is dependent on the shear rate by equation (1).[1]

$$\mu = \mu_0 + (\mu_0 - \mu_\infty)(1 + (\lambda\dot{\gamma})^a)^{(n-1)/a} \quad (1)$$

At low shear rates, the fluid acts as a Newtonian fluid with viscosity μ_0. At high shear rates, the fluid acts as a Newtonian fluid with viscosity μ_∞. For frog saliva, this high shear rate is exceeded during impact with prey. When a frog retracts its tongue, it is pulling perpendicular to the saliva and thus the saliva experiences a very low shear rate.[4] This indicates that one can treat the problem of fluid flow during prey capture as a Newtonian fluid flow problem in two phases, with a different Newtonian fluid for each. Figure 2 demonstrates the shear thinning behavior of frog saliva and has labelled each region. It is clear from this that before and after the transition region, the viscosity is constant, and the saliva can thus be treated as a Newtonian fluid.

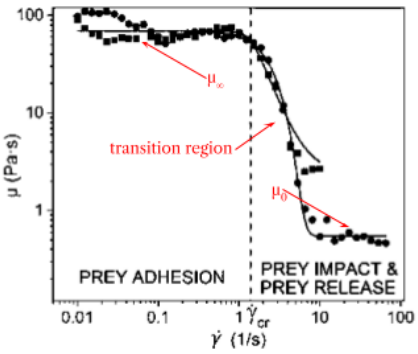

Figure 2: Viscosity vs. Shear Rate Graph of Frog Saliva[1]

1.4 An Overview of Dimensional Analysis

Most practical fluid flow problems are too complex to be solved analytically and must be solved experimentally or computationally, and the problem of adhesion in the tongue of a frog is no exception. In order to do so practically, the complexity and quantity of experimental variables affecting a phenomenon must be reduced. Dimensional analysis does this and provides scaling laws which allow data to be converted between the model and the real world.

The result of dimensional analysis is that a dimensional equation, that is, an equation containing some or all of the four basic dimensions: time, length, temperature, and [mass or force], is reduced to its non-dimensional form. This non-dimensional form will contain non-dimensional numbers which are groupings of variables. These must be held constant between the model and the real world for the results of the experiment to be able to give useful data which can be scaled. [5]

1.5 The Non-Dimensional Navier-Stokes Equation

Due to funding constraints, neither live frogs nor deceased frogs were able to be used in this research, thus it was necessary to develop a dynamically similar model which would act as a viable substitute.

The Navier-Stokes equation is the momentum equation for viscous fluid flow. To ensure that a viscous flow is comparable between nature and a model, one must have similarity in the Navier-Stokes equation. This can be done using dimensionless parameters.

At Mach numbers less than .3 the Eckert number is of negligible importance. The Mach number of the impact velocity of the frog tongue is well below this at ~.012.[4] The same can be said of the Prandtl number in situations where heat transfer is negligible. For these reasons and the fact that the continuity equation has no dimensionless parameters, this experiment is free to neglect both the continuity and energy equations.

As demonstrated in the above paragraphs, not all dimensionless numbers will need to be matched for this experiment, and indeed it is ideal if some are irrelevant in order to keep the complication of the experiment to a minimum. Therefore, a form of the Navier-Stokes equation was selected where relevant numbers would be at a minimum, while still applying to open flows.

Equation (2) is one non-dimensional form of the Navier-Stokes equation where a superscript * represents non-dimensional versions of the variables.[6]

$$\rho^* - \frac{DV^*}{Dt^*} = \frac{1}{Fr}\rho^* - \nabla^*\rho^* + \frac{1}{Re}\nabla^* \cdot \left[\mu * \left(\frac{du^*_i}{dx^*_j} + \frac{du^*_j}{dx^*_i}\right)\right] \quad (2)$$

The Reynolds number and the Froude number are defined by equations (3) and (4) respectively and are Re and Fr in equation (2).

$$Re = \frac{\rho UL}{\mu} \quad (3)$$

$$Fr = \frac{U^2}{gL} \quad (4)$$

U is the speed of fluid flow, L is a characteristic length, μ is the dynamic viscosity of the fluid, ρ is the density of the fluid, and g is the acceleration of gravity.

The Reynolds number is the ratio of inertial forces to viscous forces. The Froude number represents the effect of gravity on the motion of the fluid. At Froude Numbers greater than 1, the flow is supercritical, and disturbances cannot travel upstream.

Due to the very high values of the Froude Number for the frog's saliva flow in nature (see section 2.2 Numerical Values) and the fact that the Froude number matters for open flows (which this is not), it will not be necessary to match the Froude Number, simply to keep it similarly large.

In order to achieve dynamic similarity in the experiment to the natural process, only the Reynolds number must be matched. It must also be noted that the Froude number is only of importance if there is a free surface in the flow. [6]

1.6 The Non-Dimensional Boundary Conditions

On the frog tongue itself, a non-slip condition can be assumed both for the impact phase and the pulling phase. On the prey item, this is more complicated. For the retraction phase, it was determined that after the initial change in direction, the saliva detaches in a linear manner.[3] This is a boundary condition of the second kind where the normal derivative of the dependent variable is specified.[7] For this phenomenon, the dependent variable is position, and this normal derivative is the rate of radial detachment which is constant.

The boundary conditions also contain dimensionless parameters which must be held constant to ensure similarity of the flow. This phenomenon does not involve slip, variable temperature, free convection, or boundary heat transfer. It does have free surface conditions which introduces the Weber and Cavitation numbers. The cavitation number is important when the free stream pressure is interpreted as the vapor pressure of the liquid, which is not the case here. The Weber number is important at the interface between two fluids (in this case saliva and air) and represents the ratio of inertia to surface tension. The Weber number is important if it is small, of order 10 or less.[6] As will be seen in Numerical Values, this is not the case here.

The only number of importance ends up being the Reynolds number, and this can be matched using different plate diameters and separation velocities.

1.7 Adhesive Bond Strength Testing

In order to determine the prey capturing capabilities of the frog, it is important to get a complete picture of the bond between tongue and prey.

Adhesive strength can be mechanically modelled as the work of adhesion where F_A is the instantaneous force of adhesion and ds is an infinitesimal length parallel to the force.

$$S_A = \int F_A \cdot ds \tag{5}$$

The work of adhesion is the work required to separate a unit area of the adhering surfaces, the greater the work of adhesion, the greater the strength of the adhesive bond. This would be the ideal way to determine the adhesive strength of frog saliva adhering to surfaces of different roughnesses.

A plate separation device uses constant force to separate two plates which have been bonded by an adhesive and determines the distance at which the adhesive breaks. The work of adhesion can then be obtained by multiplying these values together.

1.8 Sandpaper Roughness Values

Since the bond between tongue and prey is what facilitates capture, it stands to reason changes on the prey surface may affect the strength of this bond.

The roughness of a surface is commonly measured using Ra, which is the arithmetic average of the roughness profile, which is determined by how far peaks and valleys of the surface are from the mean line.[8] For sandpaper of a known grit, these values are readily available.

Grit	60	80	120	150	180	220
R_a (μm)	2.21	1.80	1.32	1.06	0.76	0.48

Table 1: Grit Value and Corresponding Arithmetic Mean of Height Deviations from Main Line (Ra)

2. Experimental Methods

2.1 Materials

The following table lays out the materials used for this research and what they were used for.

Material	**Purpose**
30 count 5/16” ID washers	Plate surface
30 count .8 x 20 mm flat head metric screws	Plate fastening
Sandpaper in grits ranging from 60 to 220	Synthetic prey surface
JA-RU giant snap hand, proprietary polymer	Synthetic tongue
J-B Weld two part quick setting epoxy	Adhere non-wood materials
Titebond professional strength wood glue	Adhere wood
Plywood in thicknesses of ¼”, ⅛”, and 1/16”	Frame, piston, and tongue plate mount
1.5’ x 1” x ½” block of balsa wood	Rack mount
1’ gear rack*	Linear motion
round bore pinion gear, 24 teeth*	Connect motor to rack
ROBOTZONE 460RPM Micro Gearmotor (50:1 ratio)	Convert power into motion
DC power supply	Provide power
Drill switch	On/off for device
1080p/60FPS camera	Recording data
Physlet’s Tracker Video Analysis and Modeling Tool	Analyzing data
Pure Honey (Pasteurized)	Synthetic saliva

Table 2: Materials and Their Purposes

*all gears are 20 degree pressure angle, 48 pitch.

2.2 Numerical Values

Previous research done on horned frogs and leopard frogs provides rough values which can be used for average conditions in nature for the frog capturing prey, this will allow for a dynamically similar model to be designed and then built and tested.

A superscript of [a] on a table indicates the data was obtained from the leopard frog,[1,2] and a superscript of [b] indicates the data was obtained from the horned frog.[3,4]

The flow speed is the free stream speed of the saliva, and is assumed to be the speed of the frog tongue. The length is the characteristic length of the object in the flow i.e. the insect. The fluid density is the density of the saliva, which is assumed incompressible[2] and approximated to slightly over the density of plain water. The dynamic viscosity is the viscosity of the saliva under high and low shear stress respectively.

The first puzzle numerical values allow to solve is that of the necessity of the Weber number. The following table displays the values in nature for frog saliva upon an insect:

	Flow Speed (U) [m/s]	**Length (L)** [m]	**Fluid Density (ρ)** [kg/m^3]	**Surface Tension Coefficient (τ)** [N/m]
Highest Values or Constant at 20℃	4.0[3]	order of 10^{-2}	1000	0.0728

Table 3: Weber Number Inputs, Real World Data

Using this table and equation (5), the Weber number is calculated to be $219780.22L$ which will be on the order of 2197.8 and will certainly not reduce to 10 for an insect being captured by a frog.

$$We \equiv \frac{\rho U^2 L}{\tau} \tag{5}$$

The following tables are used for the purposes of calculating the Reynolds and Froude numbers for the phenomenon in nature. Tables 4 and 5 collect the inputs for Froude and Reynolds numbers from nature. Table 6 collects the calculated Reynolds and Froude numbers using the data in the previous two tables.

		Flow Speed (U) [m/s]	Dynamic Viscosity (μ) [Pa*s]
Impact	*(upper limit)*	4.0[a]	1.2[a]
Impact	*(lower limit)*	4.0[a]	.55[a]
Retraction	*(at insect start)*	0	70[a]
Retraction	*(midpoint)*	4.2*	70[a]
Retraction	*(at mouth)*	8.4*	70[a]

Table 4: Froude and Reynolds Number Variable Inputs

*Values obtained using a constant maximum acceleration of 120 m/s and a time of flight of .07 seconds.

	Length (L) [m]	Acceleration of gravity (g) [m/s^2]	Fluid Density (ρ) [kg/m^3]
Impact and Retraction	10^{-2}**	9.81	1000

Table 5: Froude and Reynolds Number Constant Inputs

**Value is assumed as a general approximation of insect size so that the dimensionless numbers can be calculated.

		Reynolds Number	Froude Number
Impact	*(upper limit)*	$333.\underline{3}$	163.0988787
Impact	*(lower limit)*	$72.\underline{72}$	163.0988787
Retraction	*(at insect start)*	0	0
Retraction	*(midpoint)*	.6	179.8165138
Retraction	*(at mouth)*	1.2	719.266055

Table 6: Froude and Reynolds Number at Impact and Retraction

2.3 Plate Construction

Washers were filed on the inner diameter with a rat tail file until they were flush with the heads of the flat head screws. The washers and screws were then laid concentric and flush, flat on a strip of packing tape. A two-part quick setting epoxy was mixed for 60 seconds and squeezed into the space between each washer and screw using a spreader.

To construct each prey plate, epoxy was spread thinly over one of the pre prepared washer/screw plates, and an equal diameter circle of sandpaper was adhered. Two prey plates were constructed for each grit of sandpaper incase of unforeseen damages.

To construct the tongue plates, a plate size circle was cut from a large sticky hand toy and adhered with the two-part epoxy using the method described for the prey plate.

2.4 Plate Separation Device Construction

The plate separation device uses the rack and pinion gears to transform rotational motion from a constant torque motor into linear motion. This linear motion is applied to separate the two plates with constant force.

The rack gear was adhered centered to the block of wood using the epoxy used in plate construction. Two 1”x1”x1/16” pieces of plywood were wood glued so their grains ran perpendicular and viced for 24 hours. One edge was wood glued to the end of the rack gear, and a tongue plate was epoxied to the opposite edge, and this structure was strapped down onto a table to ensure flush bonds.

An enclosure was then created which surrounds the rack gear, with a slit through the top to allow the 1”x1”x⅛” platform of the tongue plate through. This functions as a piston and holds the tongue apparatus steady. A hole was cut in the bottom of the enclosure just big enough to allow the 24-tooth pinion gear to engage with the rack gear. A platform was epoxied under this, which the motor attached to the opinion gear can be attached to.

The motor was soldered to the trigger switch mechanism of a drill, and this mechanism was soldered onto the attachment points of the power supply, which when reasonably charged provides a constant voltage, ensuring the constant torque required for this experiment.

A metric ruler the length of the piston was glued flush to the device in order to allow software to track position during the analysis of the videos in the testing procedure.

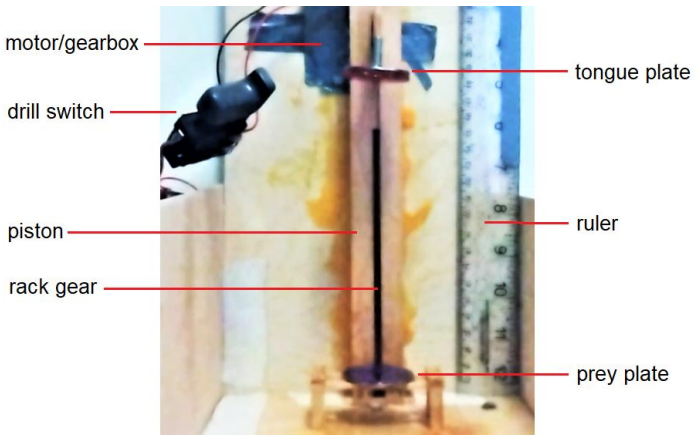

Figure 3: Exterior of plate separation device at maximum separation.

2.5 Sample Preparation and Testing

¼ teaspoon of honey was measured out and flipped over the prey plate, allowed to run for exactly five seconds to ensure the same amount of honey with each trial. The tongue plate lowered onto the prey plate and pressed down firmly.

The motor was affixed to its platform, and the camera was set up 3 feet away, parallel to the linear path of the mechanism. The camera was turned on and began to record video

At exactly five minutes past when the honey was poured, the switch was quickly lowered to its resting position, and left running until the end of the rack gear's cycle.

2.6 Video Analysis

To determine the work required to separate a "prey" plate from a "tongue" plate, the video from the high-speed camera was analyzed using Tracker.

The ruler glued to the plate separation device was set in Tracker as a calibration stick with a length of .3 meters. This was used by the software to determine the path length between plate locations frame to frame.

The point mass to track was selected to be the reflection between the screw and the washer, which was consistent in each frame. The software then tracked that reflection throughout the retraction of the tongue plate. See Figure 4 for an example of motion tracking in progress. Occasionally, the reflection would change appearances slightly and the position would have to be tracked manually in those frames.

Figure 4: Reflection locations as determined by Tracker

The path length was recorded for each frame, and from that the program derived speed and magnitude of acceleration. These were plotted, and the program took the area under the curve to determine the work.

3. Results and Discussion

3.1 Generalized Flow Behavior

Prior to the experiment, it was hypothesized that the honey would have two phases: An initial adhesive phase where the honey would be observed between the two plates getting thinner and thinner, until the detachment phase where the adhesion would be negligible.

The honey between the plates was observed to have three phases.

The first, or stationary phase, was a highly adhesive phase where the motor was running but the plates were not moving enough to be significantly detectable.

The second phase, or separation phase, involved a rapid increase in velocity not detectable by the naked eye during which the plates fully separated from one another. This jump in velocity can be seen in Figure 5, and be further understood in Figure 6.

During the third phase, or separated phase, the velocity was not significantly changing, and the plates were fully separated with no flow observed between them.

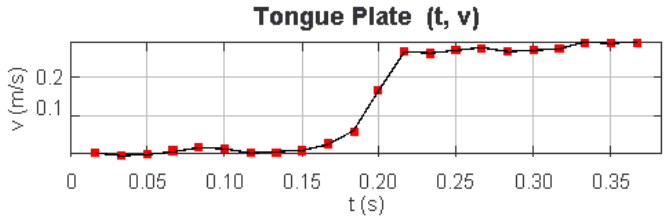

Figure 5: Velocity-time curve, 80 grit first trial.

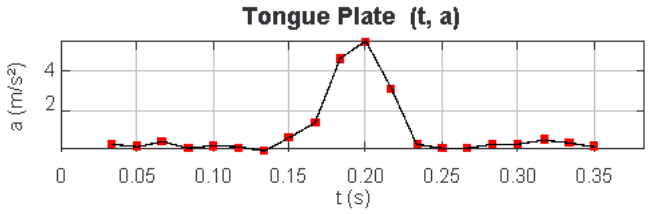

Figure 6: Acceleration-time curve, 80 grit first trial.

All plates separated at roughly the same distance, which is to say that in each trial the separation of the honey into two separate flows occurred while the plates were so close as for the flow to not be visible from an outside perspective.

For the mechanism to go up without being adhered to a prey plate, the velocity profile was different enough to indicate that it was not simply friction or the motor which is behind the data above. Instead of a jump over the span of .05 seconds, a more gradual increase in velocity occurred over the course of approximately .15 seconds. Additionally, there was no initial adherence phase where the plate was stationary. See Figure 7 for an example.

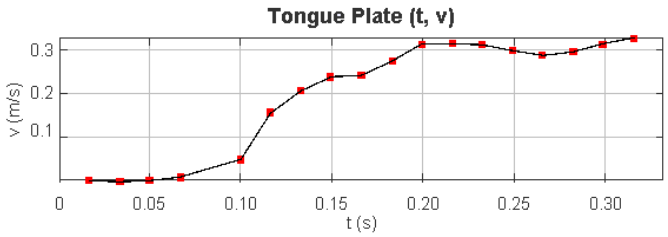

Figure 7: Velocity-time curve, no adhesion.

3.2 Impact of Surface Roughness

The parameter used to determine the impact of surface roughness on the adhesive strength was the work done during the separation phase. To do this, the area under the acceleration-displacement curve was taken for each trial of each grit value. This area is demonstrated in blue for the first trial of 80 grit sandpaper in Figure 8. The area under this curve is equal to the work divided by the mass of the accelerating object. In this case, the accelerating object is the tongue and rack gear configuration seen in Figure 3.

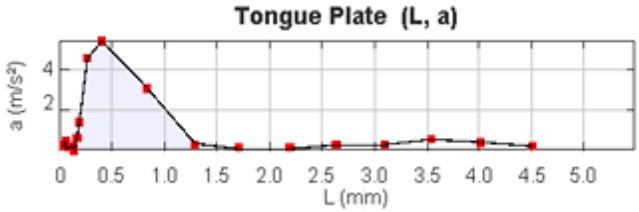

Figure 8: Acceleration-displacement curve, 80 grit first trial.

Note that because the acceleration peak happens very close to the surface of the prey plate, the acceleration peak is not towards the center of the graph.

The impact of surface roughness ultimately could not be determined using the resources available for this project. As can be seen in the Figure 9, there was no significant pattern between trials, nor was there consistency between trials.

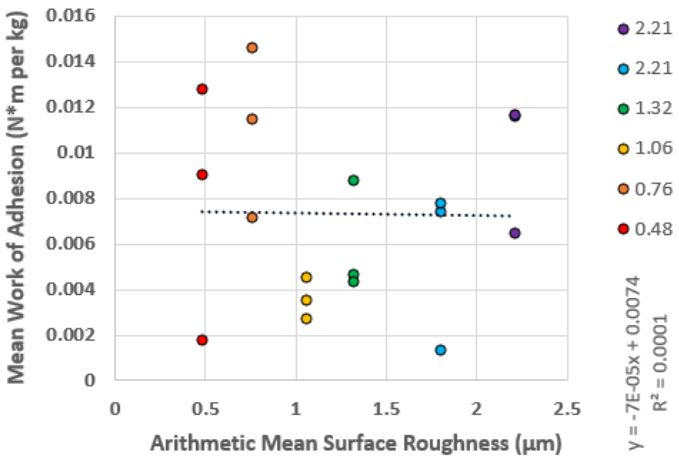

Figure 9: Mean Work of Adhesion vs. Arithmetic Mean Surface Roughness

The standard error for each grit of sandpaper made up a high percentage of the actual data value, up to 41% for 220 grit sandpaper. With an error this high, and no discernable pattern, it was clear before doing the Analysis of Variables that there would be no statistically significant correlation between surface roughness and the work done by adhesion.

Data Summary				
Group	N	Mean	Std. Dev	Std. Error
60 Grit	3	9.93	2.99	2.09
80 Grit	3	5.53	3.62	1.72
120 Grit	3	5.93	2.47	1.43
150 Grit	3	3.59	0.91	0.52
180 Grit	3	11.1	3.73	2.15
220 Grit	3	7.88	5.6	3.23

Table 7: Summary of Collected Data

A One-way ANOVA was run[9], and the results confirmed what could be inferred from Table 5 and Figure 6. The important numbers to look at for the purposes of this experiment are the F-Stat and the P-Value. Neither are significant even at the 15% probability, which is to say that there is a greater than 15% likelihood these results could be obtained from random data. There is therefore no evidence provided by this data that surface roughness influences the adhesive capabilities of the frog tongue.

ANOVA Summary					
Source	Degrees of Freedom	Sum of Squares	Mean Square	**F-Stat**	**P-Value**
Between Groups	5	121	24.2	**1.96**	**0.16**
Within Groups	12	148	12.4		
Total	17	269			

Table 8: Summary of Analysis of Variables

3.3 Sources of Error

The inability to determine the impact of surface roughness could be because surface roughness does not play a role in the adhesive properties, but it could also be due to the not insignificant sources of error and noise in this experiment.

The testing environment was not climate controlled and was a different ambient temperature during several of the trials. The plate separation device is rudimentary and imprecise. The camera (while high speed) did not have a high enough frame rate or resolution to determine what is really happening within the flow. The acceleration event took place on the order of a tenth of a second for all trials, which is approximately 6 frames. This provides only 6 data points from which to gather information, and this impreciseness is amplified each time a derivative is taken, in this case twice to obtain acceleration.

4. Conclusion

This Major Qualifying Project aimed to determine the effect surface roughness could have on the adhesive strength of a frog's tongue in order to more fully understand how it works, and how it could be potentially applied to synthetic capture mechanisms. The dependance of the adhesive strength of frog saliva on prey surface roughness was not demonstrated in this experiment. The results indicate that the device used was not sensitive enough to provide a reasonable understanding of the flow on the scale necessary. Future steps should include using a sensitive instrument and determining the role roughness has in the spread of frog saliva over the surface, as this would impact the area of adhesion.

Literature Cited

[3] Kleinteich, T., & Gorb, S. (2014, June 12). Tongue adhesion in the horned frog Ceratophrys sp. Retrieved from https://www.ncbi.nlm.nih.gov/pmc/articles/PMC5381498/

[4] Kleinteich, T., & Gorb, S. (2015, September 30). Frog tongue acts as muscle-powered adhesive tape. Retrieved from https://www.ncbi.nlm.nih.gov/pmc/articles/PMC4593688/

[2] Noel, A. C. (2018, August 01). Grip, grab and groom: The biomechanics of frog and cat tongues. Retrieved from https://smartech.gatech.edu/handle/1853/61623

[1] Noel, A., Guo, H., Mandica, M., & Hu, D. (2017, February). Frogs use a viscoelastic tongue and non-Newtonian saliva to catch prey. Retrieved from https://www.ncbi.nlm.nih.gov/pmc/articles/PMC5332565/

[7] Papanastasiou, T. C., Georgiou, G. C., & Alexandrou, A. N. (2000). *Viscous fluid flow*. Boca Raton, FL: CRC Press.

[8] Jun Qu & Albert J. Shih (2003) Analytical Surface Roughness Parameters of a Theoretical Profile Consisting of Elliptical Arcs, Machining Science and Technology, 7:2, 281-294, DOI: 10.1081/MST-120022782

[5] Szirtes, T., & Rózsa, P. (2011). *Applied dimensional analysis and modeling*. Amsterdam: Butterworth-Heinemann.

[6] White, F. M. (2006). *Viscous fluid flow*. New York, NY: McGraw-Hill.

[10] White, F. M. (2016). *Fluid mechanics*. New York, NY: McGraw-Hill Education.

[9] Winer, B. J., Brown, D. R., & Michels, K. R. (1991). *Statistical Principles in Experimental Design.* New York, NY: McGraw-Hill Education.